

Low-overhead fault-tolerant error correction scheme based on quantum stabilizer codes

Xiu-Bo Chen(陈秀波), Li-Yun Zhao(赵立云), Gang Xu(徐刚), Xing-Bo Pan(潘兴博), Si-Yi Chen(陈思怡), Zhen-Wen Cheng(程振文), and Yi-Xian Yang(杨义先)

Citation: Chin. Phys. B, 2022, 31 (**4**): 040305. DOI: 10.1088/1674-1056/ac3817
Journal homepage: http://cpb.iphy.ac.cn; http://iopscience.iop.org/cpb

What follows is a list of articles you may be interested in

Quantum watermarking based on threshold segmentation using quantum informational entropy

Jia Luo(罗佳), Ri-Gui Zhou(周日贵), Wen-Wen Hu(胡文文), YaoChong Li(李尧翀), and Gao-Feng Luo(罗高峰)
Chin. Phys. B, 2022, 31 (**4**): 040302. DOI: 10.1088/1674-1056/ac2803

Quantum simulation of lattice gauge theories on superconducting circuits: Quantum phase transition and quench dynamics

Zi-Yong Ge(葛自勇), Rui-Zhen Huang(黄瑞珍), Zi-Yang Meng(孟子杨), and Heng Fan(范桁)
Chin. Phys. B, 2022, 31 (**2**): 020304. DOI: 10.1088/1674-1056/ac380e

Fast qubit initialization in a superconducting circuit

Tianqi Huang(黄天棋), Wen Zheng(郑文), Shuqing Song(宋树清), Yuqian Dong(董煜倩), Xiaopei Yang(杨晓沛), Zhikun Han(韩志坤), Dong Lan(兰栋), and Xinsheng Tan(谭新生)
Chin. Phys. B, 2021, 30 (**7**): 070310. DOI: 10.1088/1674-1056/abff2b

Universal quantum circuit evaluation on encrypted data using probabilistic quantum homomorphic encryption scheme

Jing-Wen Zhang(张静文), Xiu-Bo Chen(陈秀波), Gang Xu(徐刚), and Yi-Xian Yang(杨义先)
Chin. Phys. B, 2021, 30 (**7**): 070309. DOI: 10.1088/1674-1056/ac003b

Encoding entanglement-assisted quantum stabilizer codes

Wang Yun-Jiang,Bai Bao-Ming,Li Zhuo,Peng Jin-Ye,Xiao He-Ling
Chin. Phys. B, 2012, 21 (**2**): 020304. DOI: 10.1088/1674-1056/21/2/020304

Low-overhead fault-tolerant error correction scheme based on quantum stabilizer codes

Xiu-Bo Chen(陈秀波)[1,†], Li-Yun Zhao(赵立云)[1], Gang Xu(徐刚)[2,3], Xing-Bo Pan(潘兴博)[1], Si-Yi Chen(陈思怡)[1], Zhen-Wen Cheng(程振文)[1], and Yi-Xian Yang(杨义先)[1]

[1] *Information Security Center, State Key Laboratory of Networking and Switching Technology, Beijing University of Posts and Telecommunications, Beijing* 100876, *China*
[2] *School of Information Science and Technology, North China University of Technology, Beijing* 100144, *China*
[3] *Advanced Cryptography and System Security Key Laboratory of Sichuan Province, Chengdu* 610025, *China*

(Received 21 October 2021; revised manuscript received 8 November 2021; accepted manuscript online 10 November 2021)

Fault-tolerant error-correction (FTEC) circuit is the foundation for achieving reliable quantum computation and remote communication. However, designing a fault-tolerant error correction scheme with a solid error-correction ability and low overhead remains a significant challenge. In this paper, a low-overhead fault-tolerant error correction scheme is proposed for quantum communication systems. Firstly, syndrome ancillas are prepared into Bell states to detect errors caused by channel noise. We propose a detection approach that reduces the propagation path of quantum gate fault and reduces the circuit depth by splitting the stabilizer generator into X-type and Z-type. Additionally, a syndrome extraction circuit is equipped with two flag qubits to detect quantum gate faults, which may also introduce errors into the code block during the error detection process. Finally, analytical results are provided to demonstrate the fault-tolerant performance of the proposed FTEC scheme with the lower overhead of the ancillary qubits and circuit depth.

Keywords: fault-tolerant error correction, quantum stabilizer code, gate fault, quantum circuit

PACS: 03.67.Pp, 03.67.−a, 03.67.Hk **DOI:** 10.1088/1674-1056/ac3817

1. Introduction

Since quantum information is affected by noise during channel transmission, a technique is needed that can correct the noise in the channel and ensure the correct transmission of the information. Shor[1] first proposed that errors in quantum information can be correctly corrected by a quantum error-correcting code (QECC). At the same time, he designed the code $[[9,1,3]]$, which requires nine qubits to encode a logical qubit and corrects any single-qubit error. Subsequently, through the classical error correction code, Calderbank, Shor, and Steane[2,3] proposed a new QECC scheme CSS (Calderbank–Shor–Steane) code, such as $[[7,1,3]]$ code. However, the decoding process of CSS code is inefficient, since it cannot obtain the results of phase error and bit error in one step of measurement. Gottesman and Calderbank[2,4] proposed stabilizer formalism and formed a theory of stabilizer code to assemble a more available and further efficient quantum error correction code. The minor stabilizer code currently in existence is $[[5,1,3]]$ code,[5] which can correct any single-qubit error using only five qubits. However, the above-mentioned error correction codes can correct errors based on the condition that the error detection and error recovery operations can be performed entirely correctly without other errors. Detecting measurements and error recovery operations are complex quantum computations, and the hardware involved in the quantum computing process may be defective. Therefore errors may be introduced into the quantum information when the hardware fails.

A relatively straightforward route to achieving reliable computing is reducing the basic error rate of hardware during computing. However, a quantum system's basic error rate is determined by the quantum computer hardware's manufacturing quality and technical level, the interaction between the system and the environment, and the physical means of operation. Extraordinary experimental efforts in recent years have reduced the effect of the fundamental error rate on quantum systems in Refs. [6–9]. Using a QECC, Chou *et al.*[10] made the fidelity of teleported gate achieve 79%. Teleported gates have implications for fault-tolerant quantum computation. In addition to QECC, entanglement-assisted quantum error correction codes (EAQECC) have also been further investigated in Refs. [11,12], which improve the error correction capability of QECC. Then Jones *et al.*[13] asserted that a logical qubit must have four characteristics to be extensible, in addition to the DiVincenzo criteria for a quantum computer. Implementing a QECC scheme not only demands reducing the basic error rate but also should be fault-tolerant.

The superiority of QECC in fault-tolerant quantum computing was first introduced in Ref. [14]. It allows the correct quantum information to be recovered even if some errors occur during error detection and error recovery. Besides detection, the beginning application of QECC lies in

†Corresponding author. E-mail: flyover100@163.com
© 2022 Chinese Physical Society and IOP Publishing Ltd

protecting quantum information while performing calculations dynamically and in completing efficient quantum state transmission,[15,16] even by adopting defective logic gates during computation. Three representative FTEC schemes were introduced by Shor,[17] Steane[18] and Knill.[19,20] Salas *et al.*[21] made improvements such as "step" optimization, significantly reducing fault-tolerant syndrome extraction time and resource consumption. These methods have accomplished the control of the spreading error of the syndrome extraction circuit. Nevertheless, to achieve fault-tolerant syndrome extraction, it is essential to determine whether the syndrome qubits have introduced errors during the preparation process since otherwise, the errors could be propagated to the coding block.

Until 2017, Yoder and Kim[22] first proposed extracting fault-tolerant syndrome using flag qubits, which greatly reduced the consumption of ancillary qubits resources. After that, Chao *et al.*[23–27] further introduced the "flag paradigm", which works well for catching the correlated errors caused by quantum gate failures. Only two ancillary qubits are needed for various distance-three codes and $\leq d+1$ ancillary qubits for any distance-d stabilizer code. Shortly after, the flag paradigm has been given for several code families: Hamming codes,[23] rotated surface and Reed–Muller codes,[28] color codes,[28–32] cyclic CSS codes,[33,34] heavy-hexagon code and heavy-square code.[35] In addition to the above mentioned abundant quantum codes, the flag paradigm can also be instrumental in preparing specific quantum states, such as magic state.[36,37]

Concerning the problem of two distinct sources of errors, noisy channels and defective hardware, ancillary qubits are added to distinguish between the two sources of errors. In actuality, the ancillary qubits overhead can complicate the device and make it difficult to operate. Therefore, this paper proposes a low-overhead FTEC scheme for quantum stabilizer codes by applying the flag paradigm to the syndrome extraction circuit. In this scheme, the Bell state is used as syndrome ancillas for measuring the coding block to achieve error correction performance; in contrast, flags are added to verify the CNOT gate and perform error tolerance performance. This scheme reduces the overhead of ancillary qubits and the overhead of circuit depth, and the probability of storage errors occurring.

Following the introduction, Section 2 begins with the review of the action the error propagation through the CNOT gate. Then Section 3 concentrates on our FTEC scheme in error detection and fault detection. We take Hamming code $[5,1,3]$ as an example to describe our fault-tolerance scheme in Section 4. The conclusion of this paper is given in Section 5, and analytical results are presented to demonstrate the fault-tolerant performance of the proposed FTEC scheme.

2. Preliminaries

In quantum information, the quantum state is a vector in $(\mathbb{C}^2)^{\otimes n}$, and the error is a unitary linear transformation. According to the simplified model of Shor and Steane, any single quantum state error can be expressed as a combination of the X, Y, and Z errors. We only need to consider the three typical errors, X, Y, Z, where

$$X=\begin{pmatrix}0&1\\1&0\end{pmatrix},\quad Z=\begin{pmatrix}1&0\\0&-1\end{pmatrix},\quad Y=\begin{pmatrix}0&-\mathrm{i}\\\mathrm{i}&0\end{pmatrix}. \tag{1}$$

A stabilizer code is a common eigenspace of a set of commuting products of Pauli operators. A generator in stabilizer may be X-type (consisting of only Pauli X and I operators) operator, Z-type (only Pauli Z and I) operator, or mixed-type (any other combination of Pauli operators).

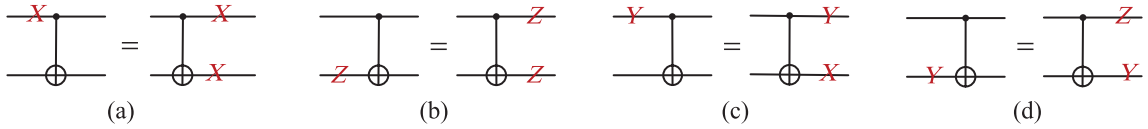


Fig. 1. (a) An X error can be propagated from the control qubit into the target qubit through the CNOT gate. (b) On the contrary, a Z error propagates from the target to the control qubit. (c) and (d) At the same time, a Y error will evolve into an X or Z error.

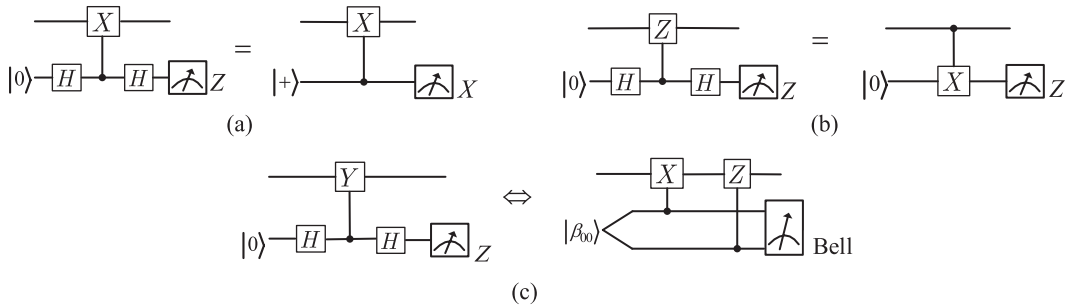


Fig. 2. The circuits of measurement of the Pauli X, Z and Y operators. (a) The circuit on the left of the equal sign uses the Z-basis to measurement, and the right uses the X-basis ($|+\rangle$,$|-\rangle$). (b) The equivalent circuit of CNOT gate and control-Z gate, finally measured with the Z-basis ($|0\rangle$,$|1\rangle$). (c) A control-Y gate can be divided into CNOT gate and control-Z gate provided that the global phase factor is ignored. The symbol "Bell" indicates a Bell basis (as in Eq. (2)) measurement. Provided an X or a Z error in the data, the measurement result will be $|\beta_{10}\rangle$. While a Y error occurs, $|\beta_{00}\rangle$ will be given.

A general error of a single qubit can be expressed as a sum of Pauli operators taken from the set $P = \{I, X, Z, Y = iXZ\}$, where I is the identity (corresponding to no error). Errors can be propagated between the target and the control qubits of a CNOT gate in Fig. 1.

Using the error transmission nature of CNOT gates to implement parity checking of a stabilizer code, extract the syndromes, locate the error type and error location, and complete error detection and correction. The error syndrome extraction is a critical step in errors detection and errors correction. The equivalent circuits of the CNOT, control-Z and control-Y are shown in Fig. 2.

The four Bell states are

$$|\beta_{00}\rangle = \frac{1}{\sqrt{2}}(|00\rangle + |11\rangle); \quad |\beta_{01}\rangle = \frac{1}{\sqrt{2}}(|01\rangle + |10\rangle);$$
$$|\beta_{10}\rangle = \frac{1}{\sqrt{2}}(|00\rangle - |11\rangle); \quad |\beta_{11}\rangle = \frac{1}{\sqrt{2}}(|01\rangle - |10\rangle). \quad (2)$$

The error transmission nature of the CNOT gate raises the possibility of error propagation, allowing severe errors to occur in the coding block, exceeding the error correction capability of the error correction code itself and producing a permanent error code. Therefore the syndrome extraction circuit needs to be fault-tolerant.

3. Flag-FTEC scheme

A delicately designed circuit can not only correct errors introduced in the noisy channel but also tolerate faults by itself. The difference between fault and error is as follows:[38] Fault is a location in a circuit where a gate or storage error occurs while error is associated with a qudit in a block that deviates from the ideal state. Fault happens at fixed points in the circuit but error may happen when the qudit is in fly. The circuit is referred to as a fault-tolerant circuit, i.e., the faults produced and propagated by the quantum gates in such a circuit are correctable. Next, we will introduce a low-overhead FTEC scheme, which not only reduces the error propagation path but also corrects the correlated errors on data.

3.1. Error detection — split each stabilizer generator into X-type and Z-type for classification measurement

When Alice sends an encoded quantum state $|\phi\rangle$ to Bob through a noisy channel, the encoded quantum state $|\phi\rangle$ is transformed into a noisy data $|\varphi\rangle = \varepsilon|\phi\rangle$, where ε is a channel noise operator. In order to correct the error ε, Bob starts to prepare Bell states $|\beta_{00}\rangle$ as syndrome qubits and uses all stabilizer generators to measure $|\varphi\rangle$. Each stabilizer generator is divided into X-type and Z-type operators. The term X-type (or Z-type) operator includes X (or Z) operator only. A stabilizer generator $g = XZZXI = X_{14}Z_{23}I_5$ illustrates this point clearly. Let letters A, B, and C denote, respectively, the set of subscripts of Pauli operators X, Z and I, then the stabilizer generator $g = XZZXI = X_{14}Z_{23}I_5$ can be depicted as $g = X_AZ_BI_C$ (usually denoted as $g = X_AZ_B$). The circuit of extracting generator $g = X_AZ_B$ syndrome is illustrated in Fig. 3. In particular, if there is no Y Pauli operator in the generator, $A \cap B = \emptyset$ and $A \cap B \neq \emptyset$ otherwise.

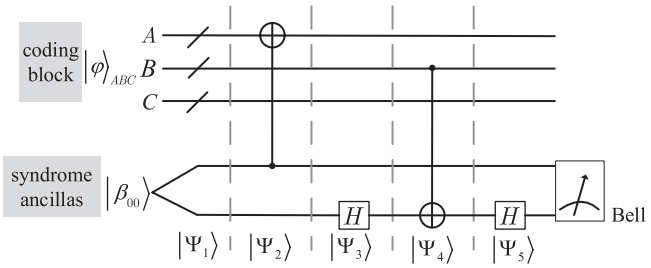


Fig. 3. Diagram for a syndrome extraction circuit that detects channel noise. A noisy data is $\varepsilon|\phi\rangle = |\varphi\rangle_{ABC}$ and syndrome ancillas are $|\beta_{00}\rangle$. Time moves from left to right, with wires used to represent the passage of time where the states are single or multiple. $|\Psi_1\rangle$, $|\Psi_2\rangle$, $|\Psi_3\rangle$, $|\Psi_4\rangle$, $|\Psi_5\rangle$ are evolution of all quantum states.

According to Fig. 3, the quantum states $|\Psi_1\rangle$, $|\Psi_2\rangle$, $|\Psi_3\rangle$, $|\Psi_4\rangle$, $|\Psi_5\rangle$ can be achieved followed by the operation of the circuit goes as follows, with the steps applied in order:

1. At first, after adding syndrome ancillas $|\beta_{00}\rangle$ the initial quantum state is
$$|\Psi_1\rangle = \varepsilon|\phi\rangle_{ABC} \otimes |\beta_{00}\rangle = |\varphi\rangle_{ABC} \otimes \frac{1}{\sqrt{2}}(|00\rangle + |11\rangle).$$
2. The quantum CNOT gates which correspond to X operators in $g = X_AZ_B$ act on the coding block, where the control qubit is the first qubit of syndrome ancillas $|\beta_{00}\rangle$ and the target qubits are data qubits A,
$$|\Psi_2\rangle = |\varphi\rangle_{ABC} \otimes \frac{1}{\sqrt{2}}|00\rangle + X_A|\varphi\rangle_{ABC} \otimes \frac{1}{\sqrt{2}}|11\rangle.$$
3. The second qubit of syndrome ancillas $|\beta_{00}\rangle$ is applied by H gate as for $Z = HXH$. The output of the H gate will be
$$|\Psi_3\rangle = |\varphi\rangle_{ABC} \otimes \frac{1}{\sqrt{2}}|0\rangle|+\rangle + X_A|\varphi\rangle_{ABC} \otimes \frac{1}{\sqrt{2}}|1\rangle|-\rangle.$$
4. Take qubits B in coding block as the control qubits and the second qubit of syndrome ancillas $|\beta_{00}\rangle$ as the target qubit. We can see that the action of the CNOT gates on the state $|\Psi_3\rangle$ is
$$\begin{aligned}|\Psi_4\rangle &= |\varphi\rangle_{ABC} \otimes \frac{1}{\sqrt{2}}|0\rangle|+\rangle + X_AZ_B|\varphi\rangle_{ABC} \otimes \frac{1}{\sqrt{2}}|1\rangle|-\rangle \\ &= |\varphi\rangle_{ABC} \otimes \frac{1}{\sqrt{2}}|0\rangle|+\rangle + g|\varphi\rangle_{ABC} \otimes \frac{1}{\sqrt{2}}|1\rangle|-\rangle.\end{aligned}$$
5. At last, the H gate is applied to the second qubit of $|\beta_{00}\rangle$
$$\begin{aligned}|\Psi_5\rangle &= |\varphi\rangle_{ABC} \otimes \frac{1}{\sqrt{2}}|00\rangle + g|\varphi\rangle_{ABC} \otimes \frac{1}{\sqrt{2}}|11\rangle \\ &= \varepsilon|\phi\rangle \otimes \frac{1}{\sqrt{2}}|00\rangle + g\varepsilon|\phi\rangle \otimes \frac{1}{\sqrt{2}}|11\rangle.\end{aligned}$$

- If generator g and channel noise operator ε commute, i.e., $g\varepsilon = \varepsilon g$,

$$|\Psi_5\rangle = \varepsilon|\phi\rangle \otimes \frac{1}{\sqrt{2}}|00\rangle + \varepsilon g|\phi\rangle \otimes \frac{1}{\sqrt{2}}|11\rangle = |\varphi\rangle_{ABC} \otimes |\beta_{00}\rangle.$$

  Once the syndrome ancillas is measured using Bell states, the coding block and the syndrome ancillas collapse respectively to $|\varphi\rangle_{ABC}$ and $|\beta_{00}\rangle$.

- If an error ε anticommutes with g, then the true state is $\varepsilon|\phi\rangle$,

$$|\Psi_5\rangle = \varepsilon|\phi\rangle \otimes \frac{1}{\sqrt{2}}|00\rangle - \varepsilon g|\phi\rangle \otimes \frac{1}{\sqrt{2}}|11\rangle = |\varphi\rangle_{ABC} \otimes |\beta_{10}\rangle.$$

  Otherwise, the state $|\Psi_5\rangle$ collapses into $|\varphi\rangle_{ABC}$ and $|\beta_{10}\rangle$. The result shows that the noise operator must exist and satisfy $g\varepsilon = -\varepsilon g$.

Through the above error detection process, we can find that it also works when the syndrome ancillas here is initialized into $|\beta_{10}\rangle$. Conversely, when the syndrome ancillas collapses into $|\beta_{00}\rangle$, then the noise operator must exist and satisfy $g\varepsilon = -\varepsilon g$.

It can be viewed from the above quantum circuit that the final syndrome ancillas measurement not only did not cause the collapse of the qubits in the coding block (data) but also copied the error in the coding block to the syndrome ancillas. Subsequently, this circuit diagram can be invoked as the circuit of syndrome extraction for data. Let $S = (s_1, \ldots, s_r) \in \mathbb{F}_2^r$ denote error syndrome of all stabilizer generators $g_1, \ldots, g_r$. Prepare syndrome ancillas in $|\beta_{00}\rangle$ to measure the ith generator followed by measuring with Bell base. If the result is $|\beta_{00}\rangle$ ($|\beta_{10}\rangle$), then the corresponding element $s_i = 0$ ($s_i = 1$). We can find that it also works when the syndrome ancillas here is initialized into $|\beta_{10}\rangle$. Conversely, when syndrome ancillas collapses into $|\beta_{00}\rangle$, the noise operator ε must exist and satisfy $g\varepsilon = -\varepsilon g$.

Above measurements must also be fault tolerant. If not, error accumulation would rapidly destroy the coherence of the states in the computer.

3.2. Fault detection — flag particles $|0\rangle$ and $|+\rangle$ are used to detect X and Z faults simultaneously

In the following subsection, we will put forward a procedure based on adding "flags" qubits to catch the quantum gate faults that can lead to correlated errors on coding block.

At first, syndrome ancillas $|\beta_{00}\rangle$ are equipped with two flags ancillas $|0\rangle$ and $|+\rangle$ with the view to increasing fault-tolerance performance as in Fig. 4. The syndrome ancillas detects errors in the coding block, and the two flags qubits can be used as a verification block. The verification block is significantly different from Shor state[17] and Steane state[18] in an essential respect that the verification block herein is not to verify whether the syndrome ancillas is prepared correctly, but to catch the faults that can lead to correlated errors on the data.

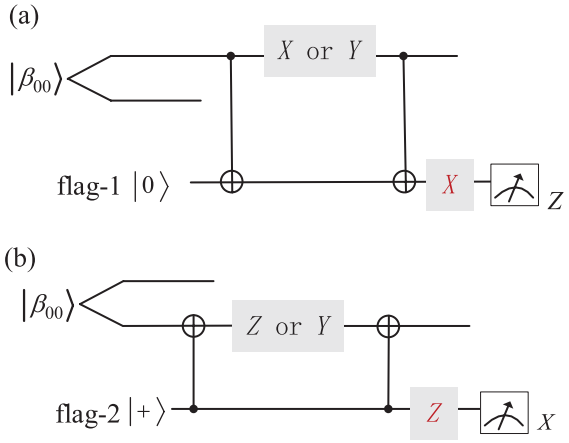


Fig. 4. Fault detection. (a) If an X or Y error is introduced to the first qubit of $|\beta_{00}\rangle$ state, the Z-basis ($|0\rangle, |1\rangle$) measurement will always give $|1\rangle$. Otherwise, $|0\rangle$. (b) If a Z or Y error occurs, the X-basis ($|+\rangle, |-\rangle$) measurement will show $|-\rangle$; otherwise, $|+\rangle$.

Then extract syndrome for stabilizer generator $g = X_A Z_B$ is shown in Fig. 5. Let X_{A_i} (or Y_{A_i}) denote as an X fault (or a Y fault) which comes from the ith CNOT gate corresponding to set A on the control qubit, where $i = 1, 2, \ldots, |A|$. And again, we can define X_{B_j} (or Y_{B_j}) as an X fault (or a Y fault) which comes from the jth CNOT gate corresponding to set B on the target qubit, where $j = 1, 2, \ldots, |B|$. In fact, the CNOT gate corresponding to the set A (B) may also introduce faults in the target (control) qubit, but the faults are not propagated to other quantum bits and therefore do not cause error multiplication.

- If there is no channel noise error (the channel noise error may commute with the generator $g = X_A Z_B$) and no quantum gate fault, the measurement results are shown in column 2 of Table 1.

- If the coding block is only affected by channel noise ε, all measurements are shown in column 3 of Table 1 when the generator $g = X_A Z_B$ anticommutes with ε.

- If an X_{A_i} or Y_{A_i} fault is introduced, the following CNOT gates will propagate the fault in A to the coding block and flag-1, causing the weight of coding block error ≥ 1 and the flag-1 raised.

  - When $A \cap B = \emptyset$, if an X (or Y) fault occurs, the measurements of syndromes ancillas is $|\beta_{01}\rangle$ (or $|\beta_{11}\rangle$).
  - When $A \cap B \neq \emptyset$, based on the quantum circuits in Fig. 2, a control-Y gate in quantum circuit can be represented as shown in Fig. 6. If an X (or Y)

fault occurs, the X error is propagated through the CNOT gate in the direction of the red arrow and the measurements of syndromes ancillas is $|\beta_{11}\rangle$ (or $|\beta_{01}\rangle$).

It is notable for its inability to distinguish between the X_{A_i} and Y_{A_i} faults by the results of Bell measurements of syndrome qubits as shown in columns 4 and 6 of Table 1. Fortunately, the X and Y faults result in the same error in the coding block regardless of whether the intersection of A and B is the empty set.

- If an X_{B_j} or Y_{B_j} fault is introduced, the following CNOT gates will propagate the fault in B to the coding block and flag-2, causing the weight of coding block error ≥ 1 and the flag-2 raised. The X_{B_j} or Y_{B_j} fault also can be identified by the results of Bell measurements of syndrome qubits. Therefore, the measurements of X_{B_j} or Y_{B_j} fault are shown in columns 5 and 7 of Table 1.

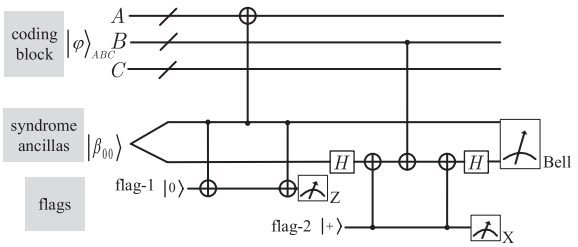


Fig. 5. Flagged syndrome extraction for stabilizer generator $g = X_A Z_B$.

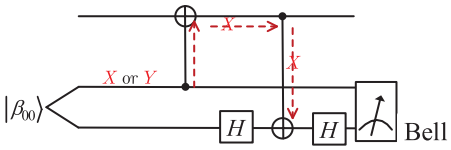


Fig. 6. Propagation of an X or Y fault through two CNOT gates acting on the same qubit. The red arrow indicates the propagation path of an X error.

The four Bell states $|\beta_{00}\rangle$, $|\beta_{01}\rangle$, $|\beta_{10}\rangle$ and $|\beta_{11}\rangle$ can realize mutual transformation under the influence of Pauli operators, i.e., $|\beta_{00}\rangle = Z^{a_i}X^{b_i}|\beta_{a_i b_i}\rangle$, where, $a_i, b_i \in \{0,1\}$, $i = 1,2,\ldots,r$. Furthermore, $|0\rangle = X^{c_i}|c_i\rangle$, $|+\rangle = Z^{d_i}\frac{|0\rangle+(-1)^{d_i}|1\rangle}{\sqrt{2}}$, where, $c_i, d_i \in \{0,1\}$. The more prominent paper by Divincezo[39] lays out "five requirements" for physically computing quantum information, one of which is the ability to initialize the state of the qubits to a simple fiducial state. Consequently, the syndrome ancillas and flags after measured can be reset to extract subsequent generators syndromes. At the terminal, extract the syndromes for all generators $g_1, g_2, \ldots, g_r$ as in Fig. 7. In particular, if there are non-trivial measurements of flags when measuring the generator g_l ($l < r$), the subsequent generators will cease measurement, and the coding block will then be re-measured using a perfect circuit and the coding block error introduced by the quantum gate fault will be corrected.

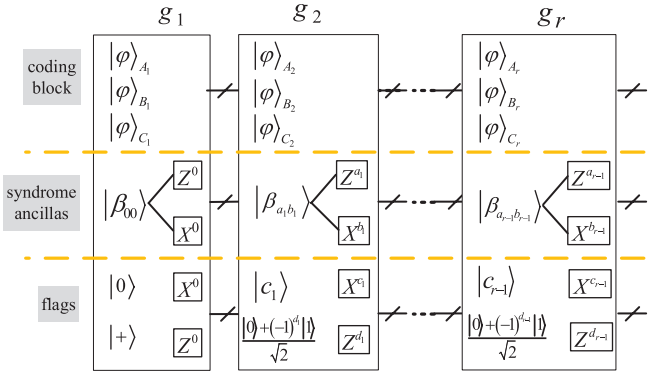


Fig. 7. The quantum measurement circuit to extract syndromes of all generators $g_1, g_2, \ldots, g_r$ in turn. The syndrome ancillas and flags are respectively initialized to $|\beta_{00}\rangle$, $|0\rangle$ and $|+\rangle$, then used to measure the generator g_1. $|\beta_{a_1 b_1}\rangle, |c_1\rangle, \frac{|0\rangle+(-1)^{d_1}|1\rangle}{\sqrt{2}}$ are the quantum states after the measurement of g_1. Output the measurement results a_1, b_1, c_1, d_1 and reset by Z^{a_1}, X^{b_1}, Z^{c_1} and X^{d_1} operators for g_2. Similarly, the measurement of generator g_r is preceded by resetting $|\beta_{a_{r-1}b_{r-1}}\rangle, |c_{r-1}\rangle, \frac{|0\rangle+(-1)^{d_{r-1}}|1\rangle}{\sqrt{2}}$ through $Z^{a_{r-1}}$, $X^{b_{r-1}}$, $Z^{c_{r-1}}$ and $X^{d_{r-1}}$ operators.

Table 1. The relationship between measurement results and CNOT gates faults.

	No error	Channel error	X_{A_i} fault	Z_{B_j} fault	Y_{A_i} fault	Y_{B_j} fault
Syndrome ancillas	$\|\beta_{00}\rangle$	$\|\beta_{10}\rangle$	$\|\beta_{01}\rangle$ (or $\|\beta_{11}\rangle$)	$\|\beta_{01}\rangle$	$\|\beta_{11}\rangle$ (or $\|\beta_{01}\rangle$)	$\|\beta_{11}\rangle$
Flag-1	$\|0\rangle$	$\|0\rangle$	$\|1\rangle$	$\|0\rangle$	$\|1\rangle$	$\|0\rangle$
Flag-2	$\|+\rangle$	$\|+\rangle$	$\|+\rangle$	$\|-\rangle$	$\|+\rangle$	$\|-\rangle$

Through the measurement results in Table 1, we can correct the errors as follows:

- If the coding block immunizes to the channel noise (or channel noise ε commutes with all generators $g_1, g_2, \ldots, g_r$) and the CNOT gate introduces no-fault, the measurement results of all ancillary quits are trivial. Therefore, the syndromes $S = (s_1, \ldots, s_r) = \mathbf{0}$.

- If the coding block is affected only by the noise channel, the measurement results of party generators are presented in the third column, the remaining are in the second column, and the quantum syndrome is $S \neq \mathbf{0}$. Finish by applying the corresponding correction.

- If flags measurement outcomes remain non-trivial, it indicates that a single CNOT gate introduces a fault propagated to the coding block. By practising "flag" ancilla, the fault type (X, Y or Z) and range (CNOT gate corresponding to set A or B) can be determined. Measure all generators with unflagged circuits (perfect) once again to figure out the position of the gate fault. If two coding block errors are affected by the failure of CNOT gates in

the same set A or B, the coding block error can be corrected when the syndromes corresponding to these two errors are different.

Through the above analysis, we summarize the whole program by a flowchart as shown in Fig. 8. Using Fig. 7 to initialize the ancillary qubits, record the measurement results based on Table 1.

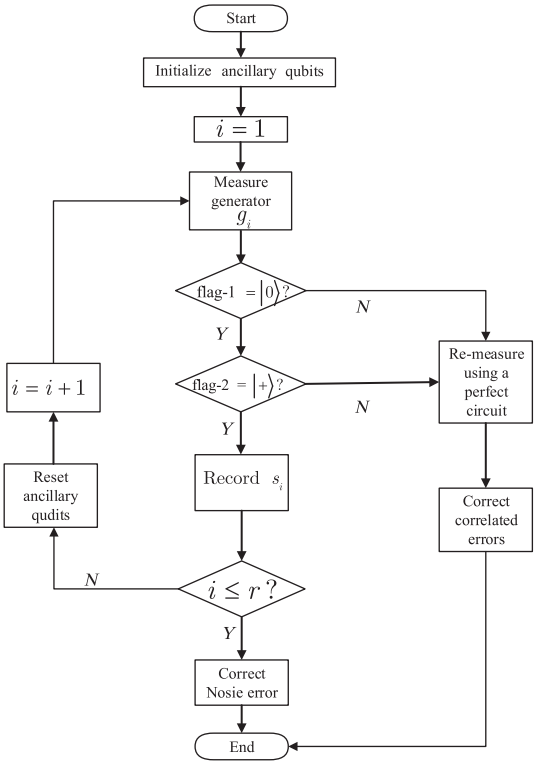


Fig. 8. A flowchart for summarizing the flag paradigm idea to realize the fault-tolerant error-correction.

Let us point out that, in our above scheme, multiple measurements are required to measure the reliability of the results, and the majority decision method is adopted to determine the ultimate result.

4. Fault-tolerance scheme for $[[5,1,3]]$ code

The most insignificant error-correcting stabilizer code $[[5,1,3]]$ can correct up to one error at any qubit[5] with stabilizer generators $g_1 = XZZXI$, $g_2 = IXZZX$, $g_3 = XIXZZ$, $g_4 = ZXIXZ$. Before the error-correction procedure, we assume that the data error weight is ≤ 1. The syndrome of g_1 can be extracted by the circuit in Fig. 9, presented by Ref. [23], where a flag can "catch" a Z fault introduced by the CNOT gate. It allows one to examine the $[[5,1,3]]$ code, single-error correcting stabilizer code, adopting two extra qubits barely. Were we to use the error-correction procedure in Fig. 9, although the quantum circuit reduces the cost of ancillary qubits, it increases the cost of circuit depth. For example, the circuit depth is 8 in Fig. 9. Besides, the Z fault will propagate through the subsequent gates and become an X-type fault. For example, provided that the gate c introduces an IZ fault, the IZ fault will be propagated through the next gate, followed by becoming an $IIIXI$ error to the data. To resolve the problem of circuit depth overhead, we practice the circuit in Fig. 9 to extract the syndrome for g_1. The flag-1 (flag-2) ancilla can "catch" the X (Z) fault simultaneously. The principal criterion between Figs. 9 and 10 lies in the syndrome ancillas and flag qubits, an essential part of fault-tolerance schemes. Figure 10 shows that the circuit depth for extracting the syndrome of g_1 is 6, which is due to the fact that a, b and c, d can run in parallel.

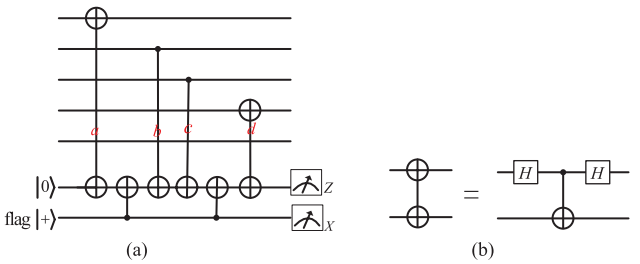


Fig. 9. (a) Flagged syndrome extraction for $g_1 = XZZXI$ in $[[5,1,3]]$ code put forward by Chao *et al.* (b) The equivalent circuit of a and d quantum gates in (a).

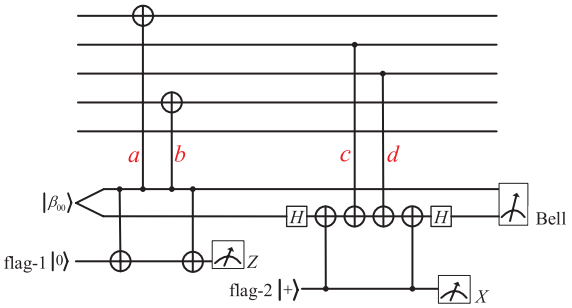


Fig. 10. Flagged syndrome extraction for $[[5,1,3]]$ code. The circuit to extract the syndrome of the stabilizer $g_1 = X_{14}Z_{23}$ with $|\beta_{00}\rangle$ state and two flag-qubits which are prepared in the $|0\rangle$ and $|+\rangle$ states. The symbols a, b (or c, d) stand for CNOT gate which correspond to sets $A = \{1,4\}$ (or $B = \{2,3\}$), respectively. The syndrome ancillas and flags are measured at the end of the circuit by Bell basis, X-basis and Z-basis.

If the data has no errors then the Bell-basis, X-basis and Z-basis measurements will always give $|\beta_{00}\rangle$, $|0\rangle$ and $|+\rangle$, respectively.

If the CNOT gate a or b fails and introduces an X (or Y) fault on control qibit, this fault will lead $|\beta_{00}\rangle$ and flag-1 ancilla to become $|\beta_{01}\rangle$ (or $|\beta_{11}\rangle$) and $|1\rangle$. Here, the 1st and 4th qubits may be suffer from errors in Table 2, where the first (second) error operator stands for the CNOT gate fault on the control (target) qubit. Use unflagged circuits to extract all four syndromes of g_1, g_2, g_3, g_4 again. It is surprised to find that the syndromes of these errors are different. Therefore, when the flag-1 ancilla is raised, the correlated errors on data are correctable by applying the corresponding correction.

In the same way, if a Z (or Y) fault stems from the controlled qubit of c or d gate the measurements will be $|\beta_{10}\rangle$ (or $|\beta_{11}\rangle$), $|0\rangle$ and $|-\rangle$. The data errors can be corrected perfectly according to data errors and syndromes in Table 2.

Table 2. The correlated errors and their corresponding syndromes.

a failure	Data error	Syndrome
XI, YI	X_4	(0,1,1,0)
XX, YX	X_{14}	(0,1,1,1)
XY, YY	Y_1X_4	(1,1,0,1)
XZ, YZ	Z_1X_4	(1,1,0,0)
b failure	Data error	Syndrome
XI, YI	I	(0,0,0,0)
XX, YX	X_4	(0,1,1,0)
XY, YY	Y_4	(1,1,1,1)
XZ, YZ	$Z4$	(1,0,0,1)
c failure	Data error	Syndrome
IZ, IY	Z_3	(0,0,1,0)
XZ, XY	X_2Z_3	(1,0,1,0)
YZ, YY	Y_2Z_3	(1,1,1,1)
ZZ, ZY	Z_{23}	(0,1,1,1)
d failure	Data error	Syndrome
IZ, IY	I	(0,0,0,0)
XZ, XY	X_3	(1,1,0,0)
YZ, YY	Y_3	(1,1,1,0)
ZZ, ZY	Z_3	(0,0,1,0)

Similarly, apply the flagged circuit to extract g_2, g_3, g_4 and followed by correcting errors based on the measurement of syndromes and flags.

5. Discussion

Both Shor's[17] and Steane's[18] FTEC schemes practice transverse fault-tolerant technology to prevent errors to cross propagation. A common feature of both schemes is the possibility of measuring all operators in a generator in parallel, but this is based on the overhead of the ancillary qubits. On the one hand, for an $[[n,k,d]]$ CSS code, the ancillary qubits costs in the above Steane's and Shor's schemes are $\geq 2(n+1)$ and $\geq 2\omega-1$ (or $\omega+1$), respectively, where ω is the maximum weight of all stabilizer generators. On the other hand, the ancilla in Shor's scheme is prepared in "cat state", while the ancilla in Steane's scheme is prepared in a superposition of all states satisfying the parity checks of $\mathcal{H}$, where each row of $\mathcal{H}$ is interpreted as a single $2n$-bit parity check. Consequently, their schemes require the preparation of syndrome ancillas into complex specific quantum states and increase circuit depth for the preparation of ancillary qubits. For example, if the Shor's and Steane's schemes are used on the $[[5,1,3]]$ code, the circuit depths for preparing the syndrome ancillas are 5 and 6, respectively. If the verification fails, the syndrome ancillas need to be re-prepared, so the overhead in the circuit depth for preparing the syndrome ancillas is $5t$ and $6t'$, where t and t' are the times of preparing the syndrome ancillas. Considering that the measurement generators can be parallelized, the total overheads of circuit depth are $T_{\text{cat}} > 5t$ and $T_{\text{Steane}} > 6t'$, respectively.

In the "flag" fault-tolerant scheme proposed by Chao *et al.*, only one syndrome qubit is used in the syndrome ancillas. Although the overhead of the ancillary qubits is reduced, it is at the cost of increasing the circuit depth. If measure the generator $g = X_AZ_B$ in Chao *et al.*'s scheme, the circuit depth overhead is $\max\{|A|+|B|\}$ (ignore the Hadamard gate). The merits of our scheme are reflected in $[[5,1,3]]$ code as in Table 3.

Table 3. The comparison of circuit depth between our scheme and Shor's, Steane's, Chao *et al.*'s schemes in $[[5,1,3]]$.

	Shor's[17]	Steane's[18]	Chao *et al.*'s[23]	Ours
Circuit depth	T_{cat}	T_{Steane}	8	6
Ancillary qubits	≥ 7 or ≥ 5[a]	≥ 10	2	4

[a]7 ancillary qubits are required for strict validation, 5 for non-strict validation.

In our scheme, the required ancillary qubits are independent of the weight and quantity of the stabilizer generator, and the ancillary states do not need to be verified as it is prepared correctly before deciding whether it can be used in the syndrome extraction circuit. Compared with Chao *et al.*'s scheme, our scheme uses the Bell state as the syndrome ancillas. The advantages of the Bell state as the syndrome ancillas are apparent, which can reduce the circuit depth and the influence of memory errors on the coding block and reduce errors propagation path. Most importantly, the scheme can be applied to any general stabilizer code provided that the errors on data can be detectable and distinguishable. It is not difficult to find that our scheme is suitable for general stabilizer codes in addition to CSS codes.

Based on the above analysis, we can see that our scheme has the following characteristics:

- The overhead of the ancillary quantum state is only 4, which is independent of the number and weight of the stabilizer generators.
- With the application of Bell states as syndrome qubits, the overhead of circuit depth for generator $g = X_AZ_B$ is reduced to $\max\{|A|,|B|\}$.
- Ancillary states are simplistic to prepare and can be reused by various generators through resetting the ancillary states when to measure coding blocks.
- Our FTEC scheme is broadly practised and is not confined to CSS codes but can further be implemented to general quantum stabilizer codes.

Acknowledgements

Project supported by the National Natural Science Foundation of China (Grant Nos. 61671087 and 61962009), the Fundamental Research Funds for the Central Universities, China (Grant No. 2019XD-A02), Huawei Technologies Co. Ltd (Grant No. YBN2020085019), the Open Foundation of Guizhou Provincial Key Laboratory of Public Big Data (Grant No. 2018BDKFJJ018).

References

[1] Shor P W 1995 *Phys. Rev. A* **52** R2493
[2] Calderbank A R and Shor P W 1996 *Phys. Rev. A* **54** 1098
[3] Steane A M 1996 *Phys. Rev. Lett.* **77** 793
[4] Gottesman D 1996 *Phys. Rev. A* **54** 1862
[5] Laflamme R, Miquel C, Paz J P and Zurek W H 1996 *Phys. Rev. Lett.* **77** 198
[6] Sung Y, Ding L, Braumüller J, Vepsäläinen A, Kannan B, Kjaergaard M, Greene A, Samach G O, McNally C, Kim D, Melville A, Niedzielski B M, Schwartz M E, Yoder J L, Orlando T P, Gustavsson S and Oliver W D 2021 *Phys. Rev. X* **11** 021058
[7] Greganti C, Demarie T F, Ringbauer M, Jones J A, Saggio V, Calafell I A, Rozema L A, Erhard A, Meth M, Postler L, Stricker R, Schindler P, Blatt R, T. Walther M P and Fitzsimons J F 2021 *Phys. Rev. X* **11** 031049
[8] Google Quantum AI 2021 *Nature* **595** 383
[9] Hao S H, Deng X W, Liu Y, Su X L, Xie C D and Peng K C 2021 *Chin. Phys. B* **30** 060312
[10] Chou K S, Blumoff J Z, Wang C S, Reinhold P C, Axline C J, Gao Y Y, Frunzio L, Devoret M H, Jiang L and Schoelkopf R J 2018 *Nature* **561** 368
[11] Wang Y J, Bai B M, Li Z, Peng J Y and Xiao H L 2021 *Chin. Phys. B* **21** 020304
[12] Lai C Y and Brun T A 2021 *Chin. Phys. B* **88** 012320
[13] Jones C, Fogarty M A, Morello A, Gyure M F, Dzurak A S and Ladd T D 2021 *Phys. Rev. X* **8** 021058
[14] Gottesman D 1998 *Phys. Rev. A* **57** 127
[15] Li J, Chen X B, Xu G, Yang Y X and Li Z P 2015 *IEEE Commun. Lett.* **19** 115
[16] Luo M X, Deng Y, Chen X B, Yang Y X and Li H H 2013 *Quantum Inf. Processing* **12** 1969
[17] Shor P W 1996 *Proceedings of 37th Conference on Foundations of Computer Science IEEE* pp. 56–65
[18] Steane A M 1997 *Phys. Rev. Lett.* **78** 2252
[19] Knill E 2005 *Phys. Rev. A* **71** 042322
[20] Knill E 2005 *Nature* **434** 39
[21] Salas P J and Sanz A L 2004 *Phys. Rev. A* **69** 052322
[22] Yoder T J and Kim I H 2017 *Quantum* **1** 2
[23] Chao R and Reichardt B W 2018 *Phys. Rev. Lett.* **121** 050502
[24] Chao R and Reichardt B W 2018 *npj Quantum Information* **4** 1
[25] Chao R and Reichardt B W 2018 *PRX Quantum* **1** 010302
[26] Chao R 2020 *Flag the Faults for Reliable Quantum Computing* (Ph.D. Dissertation) (University of Southern California)
[27] Chao R, Beverland M E, Delfosse N and Jeongwan H 2020 *Quantum* **4** 352
[28] Chamberland C and Beverland M E 2018 *Quantum* **2** 53
[29] Reichardt B W 2020 *Quantum Science and Technology* **6** 015007
[30] Baireuther P, Caio M D, Criger B, Beenakker C W J and O'Brien T E 2019 *New J. Phys.* **21** 013003
[31] Bermudez A, Xu X, Gutiérrez M, Benjamin S C and Müller M 2019 *Phys. Rev. A* **100** 062307
[32] Chamberland C, Kubica A, Yoder T J and Zhu G Y 2020 *New J. Phys.* **22** 023019
[33] Tansuwannont T 2018 *Flag fault-tolerant error correction for cyclic CSS codes* (M.S. Dissertation) (University of Waterloo)
[34] Tansuwannont T, Chamberland C and Leung D 2020 *Phys. Rev. A* **101** 012342
[35] Chamberland C, Zhu G Y, Yoder T J, Hertzberg J B and Cross A W 2020 *Phys. Rev. X* **10** 011022
[36] Chamberland C and Cross A W 2019 *Quantum* **3** 143
[37] Chamberland C and Noh K 2020 *npj Quantum Information* **6** 1
[38] Pathak A 2013 *Elements of quantum computation and quantum communication* (CRC Press Boca Raton) p. 222
[39] DiVincenzo D P 2000 *Fortschritte der Physik: Progress of Physics* **48** 771